Assessing T cell differentiation at the single-cell level

Gerlach, C.

6

EFFECTOR AND MEMORY LINEAGE DECISION OCCURS AFTER NAÏVE T CELL PRIMING

Jeroen W.J. van Heijst[1], Carmen Gerlach[1], Silvia Ariotti[1]
and Ton N.M. Schumacher[1]

[1]Division of Immunology, The Netherlands Cancer Institute, Amsterdam, the Netherlands

unpublished

Following pathogen encounter, naïve CD8 T cells give rise to both short-lived effector and long-lived memory cells. At which point during an immune response the progeny of activated T cells commit to either of these lineages remains poorly understood. Here we assessed the developmental potential of recently activated T cells, by labeling the first four daughter cell generations (D1-D4) after infection with unique genetic tags and analyzing their fate in infection-matched recipients. These experiments reveal that the vast majority of D1-D4 cells are still multipotent and give rise to both effector and memory progeny. These data indicate that signals received by downstream progeny are required for commitment to short- or long-lived fate. Lineage commitment is therefore a relatively late event in antigen-specific T cell responses.

INTRODUCTION

When a pathogen enters a host, the adaptive immune system is faced with two important tasks. The first task is to recruit as many naïve T cells as possible that have the potential to recognize the invading pathogen[1]. As activation of naïve antigen-specific T cells results in vigorous proliferation[2-4], this warrants the generation of sufficient effector cells to combat the infection. The second task is to ensure that any naïve T cell that was able to recognize the foreign invader, and therefore is of high value to the host, is clonally preserved as memory cell for potential future encounters with the same infectious agent[5]. Thus, the simultaneous generation of both effector and memory cells is required to maintain optimal fitness. At population level, ~90% of expanded antigen-specific T cells die following pathogen clearance, whereas ~10% survive and are maintained long-term. During an immune response, the progeny of activated T cells can therefore adopt two distinct fates, namely they can become short-lived effector cells or long-lived memory cells. Exactly how cells of different longevity are generated during a response is a matter of long-standing debate[6-11].

Over the years, a number of models have been proposed that aim to explain how T cell commitment to either the effector or the memory lineage is regulated. A straightforward explanation would be that different naïve T cells give rise to either effector or memory progeny. In this model, fate could either be predetermined in the naïve T cell, or be determined by the nature of the antigen-presenting cell (APC) or the time of naïve T cell priming[12-15]. However, a study by Stemberger and colleagues in which the fate of single adoptively-transferred CD8 T cells was followed, has demonstrated that a single naïve T cell can give rise to both effector and memory progeny[16]. Furthermore, by monitoring a population of naïve CD8 T cells separated by individual genetic markers, we have recently shown that under a variety of conditions, individual naïve T cells yield both lineages[17]. Thus, naïve T cells (N cells) are not committed, and commitment to effector or memory fate must therefore occur within the daughter cell generations (D cells).

Currently, there are two models describing CD8 T cell differentiation that are compatible with one naïve T cell yielding both effector and memory progeny. However, these models differ greatly in the proposed mechanism controlling fate divergence. The first model suggests that lineage commitment is an early event following antigen encounter. This model proposes that asymmetry during the first T cell division can give rise to two daughter cells with skewed differentiation potential, resulting in the proximal daughter cell giving rise to effector progeny and the distal daughter cell yielding memory progeny (bifurcative differentiation model)[8,18]. The deterministic nature of this model suggests that signals delivered by the priming APC could suffice to allow the simultaneous development of effector and memory cells, which at its most extreme implies that already the first few daughter cell generations would be lineage committed. Alternatively, a second model suggests that lineage commitment is a relatively late event following antigen encounter. This model proposes that

activated T cells differentiate in a stepwise manner, where progression towards short-lived effector fate is controlled by successive stimulation of downstream progeny by antigen or inflammatory signals (decreasing potential model)[19,20]. Despite being stochastic in nature, this model assumes memory fate as a less differentiated (and thus earlier reached) state after activation, and therefore to some extent warrants the generation of memory cells out of each activated naïve T cell. Thus, while it is clear that naïve T cells are uncommitted, it is currently not understood whether lineage commitment during a response occurs early in the first few daughter cell generations or relatively late in more downstream progeny.

In this study, we sought to determine at which point during an immune response the progeny of activated T cells commit to either short- or long-lived fate. To assess whether lineage commitment could be an early event, we labeled the first four daughter cell generations (D1-D4) after infection with unique genetic tags (barcodes)[21], and transferred these labeled D1-D4 cells into infection-matched recipient mice to analyze their fate. Barcode distributions between effector and memory populations revealed that the vast majority of these early daughter cells still displayed uniform potential to yield both short- and long-lived progeny. These data indicate that signals received by downstream progeny are required for commitment to the effector or memory lineage and lineage commitment is therefore a relatively late event in antigen-specific T cell responses.

RESULTS

Monitoring the developmental potential of early daughter cells

To assess lineage commitment of the first few daughter cell generations that arise after naïve CD8 T cell activation, we made use of the property that retroviruses only integrate into actively dividing cells[22]. In theory, by infecting a bulk population of recently activated T cells with a retroviral barcode library at a time point when T cells have undergone a maximum of four divisions, one would expect that only the cycling daughter cells become marked with these barcode sequences. The fact that each virion contains two RNA genomes raises the possibility that both daughter cells of an activated naïve T cell inherit the same barcode. However, both RNA templates appear to be required for the integration of a single DNA provirus[23,24]. In addition, a study in fibroblasts has shown that retroviruses integrate post chromosomal DNA replication, resulting in only one of the two daughters on an infected cell inheriting the provirus[25]. These studies suggest that even if the first daughter T cell generation (D1) would be lineage committed[18], our labeling strategy should reflect this by the integration of different barcode sequences. Therefore, this retroviral barcoding strategy allows the fate of the first four daughter cell generations (D1-D4) to be monitored at the single-cell level.

To study the fate of early daughter cells by retroviral barcoding we adopted an experimental setup that has previously shown fate divergence in the first daughter cell

generation (D1)[18]. To allow barcode labeling, naïve OT-I T cells were initially primed by infection of C57Bl/6 mice with *Listeria monocytogenes* expressing ovalbumin (LM-OVA, Fig. 1A). Then, after 48 hours, activated daughter cells were isolated from spleen and labeled with barcodes in vitro. Four hours later, these labeled cells were transferred into infection-matched recipient mice to allow further effector and memory cell development in vivo. Following isolation of effector and memory populations, microarray analysis of barcodes was used to determine their ancestry.

Analysis of CFSE dilution revealed that 48 hours after LM-OVA infection, OT-I T cells isolated from spleen had either not divided or had divided 1-4 times (Fig. 1B). No T cell division was detected after 24 hours (not shown); indicating that 2 days post infection is the earliest time point at which the developmental potential of early daughter cells can be assessed. Importantly, in vivo T cell activation prior to retroviral transduction at day 2 is essential for barcode-labeling, as only OT-I T cells primed by LM-OVA but not wild-type LM efficiently integrated the barcode retroviruses (Fig. 1C). These data indicate that the use of retroviruses allows the selective marking of the first four daughter cell generations (D1-D4) generated after pathogen infection *in vivo*.

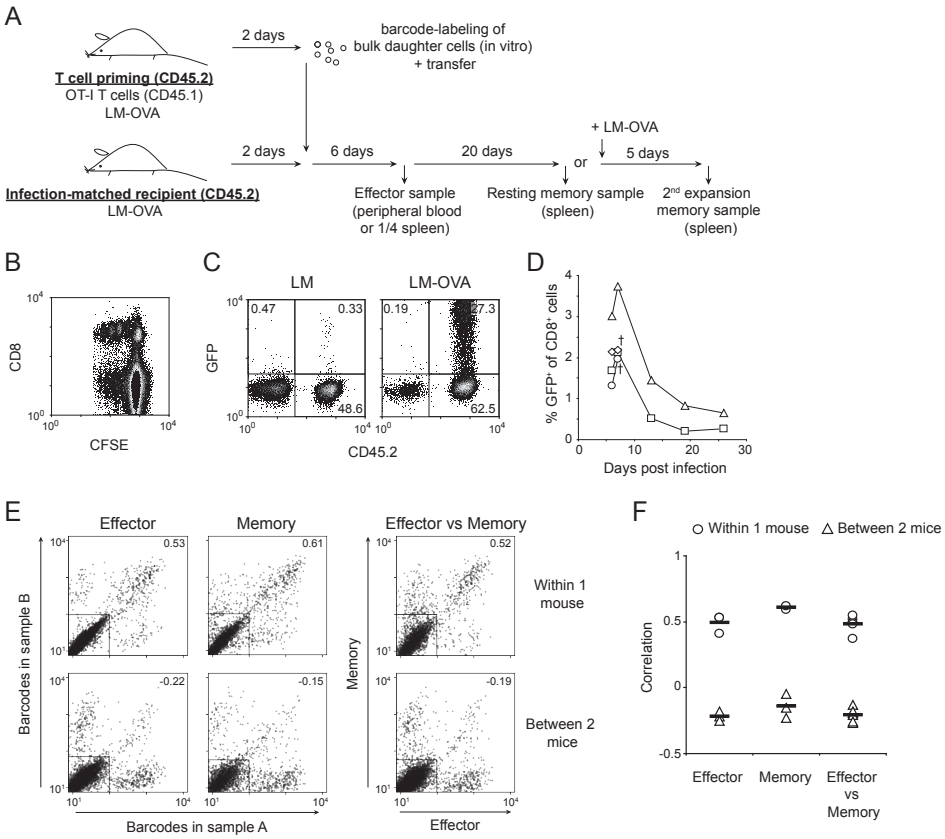

Figure 1. Developmental potential of early daughter cells. (**A**) General set-up of the adoptive transfer experiments. CD45.2 mice received 10^6 CD45.1$^+$ OT-I T cells and were infected with LM-OVA (T cell priming group). Concomitantly, CD45.2 mice were infected with LM-OVA, however without receiving any OT-I T cells (infection-matched recipient group). At day 2 post infection, spleen cells from T cell priming mice were isolated, enriched for CD8$^+$ cells, labeled with barcode retrovirus, and transferred into infection-matched recipient mice. At day 8 and 28, blood and spleen samples were obtained for barcode analysis of effector and memory populations. (**B**) CD45.2 recipients received 10^6 CFSE-labeled CD45.1 OT-I cells and were infected with LM-OVA. Flow cytometry plot, derived from spleen cells at day 2 post infection, is gated on live CD45.1$^+$ cells. (**C**) CD45.1 recipients received 10^6 CD45.2 OT-I T cells and were infected with either wild-type LM or LM-OVA. At day 2 post infection, CD8 enriched spleen cells were infected with barcode retrovirus expressing GFP and cultured for two days. Flow cytometry plots are gated on live Vα2$^+$ CD8$^+$ cells. (**D**) Following transfer of barcode-labeled daughters into infection-matched recipient mice, peripheral blood responses were tracked in time. Plot depicts the responses of four mice, of which two were sacrificed at day 7. (**E**) From infection-matched recipients, a large (~300 µl) blood sample was collected at day 8 to determine barcodes present in the effector population. From the same mice, a spleen sample was obtained at day 28 to determine barcode content of the resting memory population. Effector and memory samples were split into two halves (A and B), on which independent barcode analysis was performed. Representative barcode dot plots are shown. In these plots, each dot represents the fluorescent intensity of one barcode of the library. Rectangular dividers indicate which barcodes are present above background. Values indicate the correlation between barcode signals of sample A and B. (**F**) Correlation analysis of barcodes present in effector and memory cells of either the same or different mice.

Following transduction, CD8-purified splenocytes were transferred into infection-matched recipients and blood responses of barcode-labeled daughters were followed in time. As indicated in Fig. 1D, these responses displayed typical kinetics following acute infection; i.e. the labeled cells expanded and peaked in numbers around day 8, after which the short-lived effector cells died and the long-lived memory cells reached stable numbers around day 28. These data established that, at population level, the barcode-labeled daughters gave rise to both short-lived effector and long-lived memory cells.

To determine the kinship of these early daughter-derived effector and memory cells, a new experiment was conducted during which a large blood sample was collected at day 8 and a spleen sample was obtained at day 28, in order to analyze the barcode content of the short- and long-lived population. Each blood and spleen sample was split into two equal halves (A and B) from which barcodes were independently amplified and compared to each other. This comparison of barcodes recovered from two by definition related samples indicates how well the barcode repertoire is sampled; thereby establishing the maximum correlation that barcodes in any biologically relevant comparison can have (such as barcodes present in effector and memory populations). Likewise, barcode comparisons between two samples obtained from different mice, which are by definition unrelated, indicate the minimum correlation that barcodes from any two biologically relevant samples can have. As indicated by the barcode dot plots in Fig. 1E, barcodes present in sample A and B of the effector and memory populations were recovered reasonably well, having a mean correlation of 0.49 and 0.61 on a scale that ranges from -0.5 (completely unrelated barcodes) to 1 (completely related barcodes, Fig. 1F). Furthermore, barcodes recovered from samples of two different mice had a very low correlation (around -0.2). Interestingly, comparison of effector and memory samples revealed that most barcodes were shared, having a mean correlation of 0.48 (Fig. 1E and F). This suggests that the vast majority of D1-D4 cells is still multipotent and gives rise to both short-lived effector and long-lived memory progeny.

Kinship of primary effector and secondary expanding memory cells

Despite the fact that most barcodes between the effector and memory populations were overlapping, there were also some barcodes that were only present in either the effector or the memory sample. Although this might suggest the presence of early daughters that only gave rise to effector or memory progeny, it is difficult to firmly draw this conclusion, given that the recovery of barcodes present in the effector and memory populations was not complete. As a result, barcodes that appear unique in the effector or memory population could have been truly absent from the other population or, alternatively, could have been present but not detected.

To improve barcode recovery from effector and memory cells, we performed an experiment in which the effector sample was obtained from the spleen by partial splenectomy and the memory sample was obtained after secondary expansion,

a hallmark of memory cells. To this end, recipients of barcode-labeled OT-I daughters underwent surgery at day 8 to remove ¼ of the spleen. Subsequently, at day 28 these mice were rechallenged with LM-OVA and the remaining ¾ of the spleen was isolated 5 days later (see also Fig. 1A). Barcode analysis indicated that both effector and memory populations were efficiently sampled, with mean barcode correlations of 0.77 and 0.91, respectively (Fig. 2C and D). Importantly, barcode comparison between the well-sampled effector and memory populations showed that the majority of barcodes was overlapping, which was reflected by a mean correlation of 0.68 (Fig. 2D). Interestingly, this correlation was slightly lower than the self-self correlative values of the effector and memory comparisons, suggesting that although most effector and memory cells are progeny of the same early daughters, there might be a few clones that are already lineage committed at this early time point. Especially given the near-perfect barcode recovery of the memory population (Fig. 2C), the appearance of effector-unique barcodes, which constitute on average 23% of all recovered barcodes, might suggest that at the time of labeling some daughter cells had already lost memory potential and were destined for terminal effector differentiation.

Developmental potential of early daughter cells defined by CFSE dilution

Although a previous study in fibroblasts has shown that only half of the progeny of an infected cell inherits the proviral integration[25], the presence of two RNA genomes in each virion potentially allows both daughter cells of an activated naïve T cell to inherit the same barcode. Assuming lineage commitment in the first daughter cell generation (D1)[18], this potential double labeling could lead to false-positive kinship

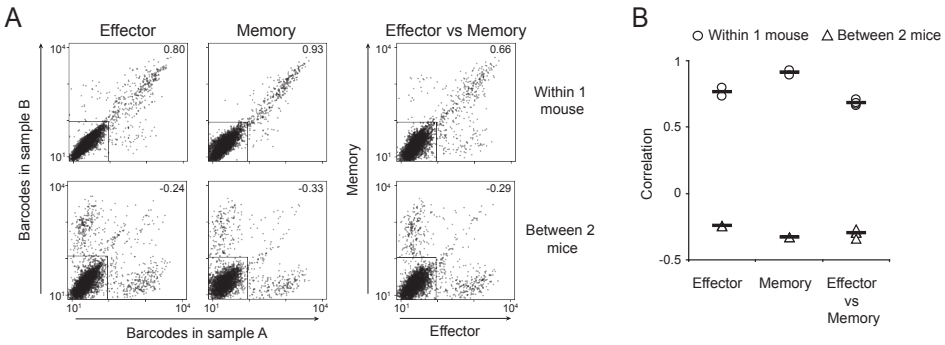

Figure 2. Early daughters give rise to both primary effector and secondary expanding memory cells. (**A**) From infection-matched recipients, a quarter spleen sample was obtained at day 8 to determine barcodes present in the effector population. The same mice were re-challenged with LM-OVA at day 28 and five days later the remaining three-quarter spleen was isolated to determine barcode content of the secondary expanding memory population. Representative barcode dot plots are shown. Values indicate the correlation between barcode signals of sample A and B. (**B**) Correlation analysis of barcodes present in effector and memory cells of either the same or different mice.

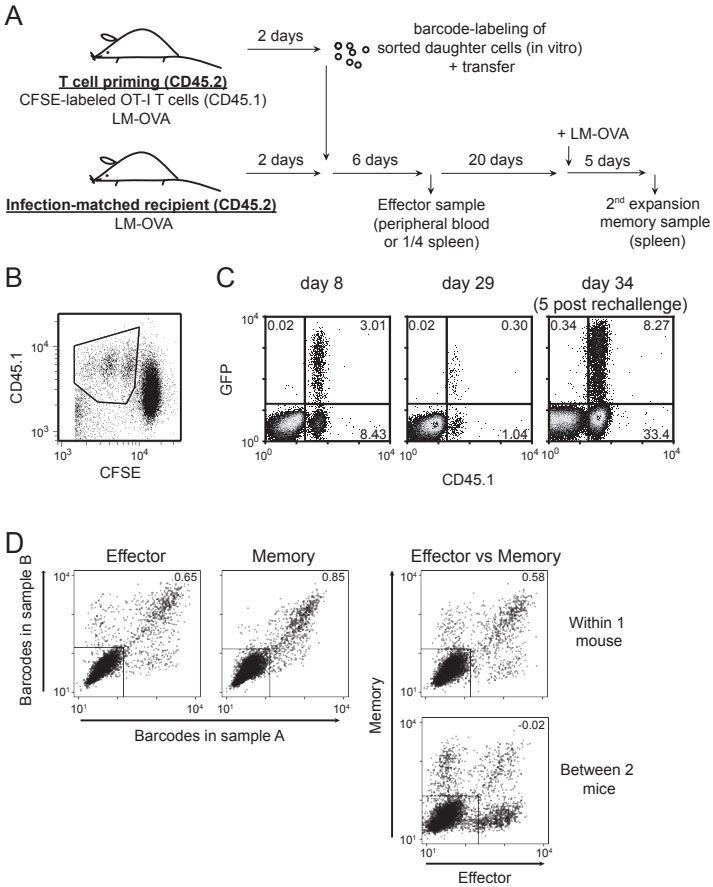

Figure 3. Effector and memory potential of sorted early daughter cells. (**A**) General set-up of the adoptive transfer experiments. CD45.2 mice received 10^6 CFSE-labeled CD45.1$^+$ OT-I T cells and were infected with LM-OVA (T cell priming group). Concomitantly, CD45.2 mice were infected with LM-OVA, however without receiving any OT-I T cells (infection-matched recipient group). At day 2 post infection, spleen cells from T cell priming mice were isolated and OT-I T cells that had divided at least once were sorted by flow cytometry. Then, sorted cells were labeled with barcode retrovirus and transferred into infection-matched recipient mice. At day 8 and 34 (5 days post rechallenge at day 29), blood and spleen samples were obtained for barcode analysis of effector and memory populations. (**B**) Flow cytometric sorting plot, gated on live CD8$^+$ T cells. Sorting gate is indicated. (**C**) Following transfer of sorted barcode-labeled daughters into infection-matched recipient mice, peripheral blood responses were tracked in time. Flow cytometry plots are gated on live CD8$^+$ T cells. (**D**) From infection-matched recipients, a large (~300 µl) blood sample was collected at day 8 to determine barcodes present in the effector population. The same mice were re-challenged with LM-OVA at day 29 and five days later a spleen sample was obtained to determine barcode content of the secondary expanding memory population. Barcode dot plots are shown. Values indicate the correlation between barcode signals of sample A and B. Note that only from one re-challenged mouse an expanding secondary memory population could be recovered and as a result no correlation plot could be generated.

interpretation of D1 cells. To address this issue we made use of CFSE dilution, to label only T cells with barcodes that have divided at least once (Fig. 3A). To this end, mice received CFSE-labeled OT-I T cells and were challenged by LM-OVA. Then, at day 2 post infection, the first 3 daughter cell generations (D1-D3) were sorted and labeled with barcodes in vitro (Fig. 3B). Four hours later, barcode-labeled daughters were transferred into infection-matched recipients to allow further differentiation into effector and memory cells. Monitoring the barcode-labeled daughters in peripheral blood indicated that these responses followed expected kinetics; i.e. the labeled cells expanded, peaked in numbers around day 8, contracted to ~10% of peak numbers around day 28 and showed enhanced expansion upon secondary antigen encounter (Fig. 3C).

From the infection-matched recipients, a large blood sample was obtained at day 8 to analyze barcodes present in the effector population. In addition, a spleen sample was obtained at day 5 post re-challenge to analyze the secondary expanding memory cells. Barcode analysis revealed that both effector and memory populations were quite efficiently sampled, with a barcode correlation of 0.65 and 0.85, respectively (Fig. 3D). Importantly, barcode comparison between the effector and memory populations demonstrated that also in this experimental setup the majority of barcodes was shared, which was reflected by a correlation of 0.58 (Fig. 3D). These data indicate that T cells, of which it was established that they had divided at least once, still retained the capacity to give rise to both effector and memory progeny. Although this behavior might be characteristic for the majority of early daughter cells, these data cannot rule out commitment of a minority of T cell clones at this early time point.

DISCUSSION

In response to infection, activated naïve T cells give rise to both short-lived effector and long-lived memory progeny. In this study, we have addressed the question at which point the progeny of activated T cells commit to the effector or memory lineage, and specifically whether an asymmetry in the first cell division could underlie this lineage decision. By labeling the first four daughter cell generations (D1-D4) that arise after infection with unique genetic tags and transferring these labeled daughters into infection-matched recipients, we were able to assess their developmental potential. These experiments revealed that the vast majority of early daughter cells were still able to yield both effector and memory progeny. A similar outcome was found, both when early daughters were labeled as a bulk activated population as well as when early daughters were labeled after CFSE-based sorting. These results indicate that the decision between short- and long-lived fate is regulated by successive stimulation of downstream progeny, suggesting that lineage commitment is a relatively late event following antigen encounter.

How can the choice between short-lived effector and long-lived memory fate then become established? A general picture that is emerging from most literature is that

continued or stronger stimulation drives cells into terminal effector differentiation, whereas more limited signaling favors the generation of memory cells (referred to as the decreasing potential model[19,20]). This stimulation typically involves to the combined effects of antigen, costimulation and cytokine signaling. Several lines of evidence indicate that when inflammation increases, this favors the generation of effector cells. For instance, sustained exposure to the pro-inflammatory cytokine IL-12 drives responding CD8 T cells into an effector phenotype[26], whereas IL-12 deficiency markedly increases memory cell generation[27,28]. Along the same note, IFN-γ is critically involved in driving successful clonal expansion and up-regulation of effector functions[29,30].

In contrast, when inflammation is restrained, this favors the generation of memory cells. For instance, when pathogen infection is terminated at a very early time point, the total number of memory cells generated remains unaltered, while effector cell numbers decrease dramatically[26,31]. Similarly, when mice are immunized by peptide-loaded dendritic cells in the absence of overt inflammation, responding CD8 T cells rapidly adopt a memory phenotype[26,32]. Further support for the notion that minimal stimulation favors memory development comes from studies on T cell homeostasis, which reported that as naïve T cells respond to lymphopenic environments, they undergo a slow homeostatic proliferation during which they progressively acquire phenotypic and functional characteristics of antigen-induced memory cells[33-35]. Interestingly, these homeostatic proliferation-induced memory cells can be equally effective at mediating protective immunity as antigen-induced "true" memory cells[36].

Another remarkable feature of memory T cell differentiation in response to antigen encounter is that it never seems to fail[10]. Both in settings with very high antigen loads and strong inflammatory signals (such as present during infection with highly virulent pathogens) as well as in settings with a relatively low degree of inflammation (such as during protein or dendritic cell immunizations), memory cells are generated[26,31]. In other words, memory cells might be generated according to a default developmental pathway that is entered as soon as a naïve T cells get activated and start to divide[37]. This observation points out a key conflict in the decreasing potential model, namely its stochastic nature. If continued stimulation selectively drives effector differentiation, how could it then be avoided that under high stimulatory conditions not all cells develop into short-lived effector cells and leave no memory cells behind? One potential explanation could be that the required level of stimulation to convert all memory precursors into short-lived effector cells is simply never reached during an immune response, because of intrinsic limitations in the availability of cytokines or APCs[12,13,38]. However, it remains difficult to reconcile a model based solely on stochastic mechanisms with the observation that the fraction of memory precursors at the peak of the primary response is more or less constant (~10%).

Intuitively, any faithful model that explains decisions between short-lived effector and long-lived memory fate should accompany a deterministic component that on one hand preserves the memory lineage, while on the other hand maintains the proper

flexibility to adjust effector cell numbers to the severity of infection. Even though a potential asymmetric division of the activated naïve T cell does not appear to lead to an immediate separation in T cell fate, it remains possible that unequal segregation of certain proteins or genetic factors renders the two daughter cells with varying susceptibility for additional stimuli at later time points. Alternatively, it could be that initial T cell divisions are symmetric, but asymmetry occurs as soon as downstream progeny have accumulated sufficient additional signaling. In fact, one might speculate that all divisions at which lineage commitment occurs are asymmetric, followed again by symmetric divisions of committed progeny to yield sufficient effector cells. For now, such models that combine features of bifurcative differentiation and decreasing potential are based on theoretical reasoning, and it remains to be experimentally determined at what point the progeny of activated T cells ultimately lose their long-lived potential as well as what factors might contribute to determining the underlying susceptibility for this event.

MATERIALS AND METHODS

Mice. C57BL/6 (B6), B6 CD45.1, OT-I T cell receptor transgenic and OT-I CD45.1 mice were bred in the animal facility of the Netherlands Cancer Institute. Mice were maintained under specific pathogen-free conditions. All experiments were performed according to institutional and national guidelines, and were approved by the Experimental Animal Committee of the Netherlands Cancer Institute.

Retroviral transduction. Retroviral supernatants were generated using Phoenix-E packaging cells as described[39] and stored at -80°C. To generate barcode-labeled daughter cells by retroviral transduction, recipients of either unmanipulated or CFSE-labeled OT-I T cells were infected with LM-OVA. After 48 hours, spleens were harvested and CD8 T cells were enriched either by magnetic bead separation (BD IMag CD8 enrichment kit), or by flow cytometric sorting based on CFSE-dilution. In case of sorting, cells were labeled by anti-CD8α-PE-Cy7 (BD, clone 53.6-7) and anti-CD45.1-APC (Southern Biotech, clone A20), and sorted on a FACSAria (BD). Purified or sorted cells were transduced with retroviral supernatant by spin infection as described[39]. Following spin infection, cells were cultured for an additional 2.5 h in retroviral supernatant. Then, cells were washed in HBSS (Invitrogen) and injected intravenously into infection-matched recipients. In some experiments, cells were cultured for two days to determine the transduction efficiency in IMDM medium (Invitrogen) supplemented with 8% heat-inactivated fetal calf serum and 100 U/ml penicillin + 100 µg/ml streptomycin (Roche), in the presence of 20 U/ml IL-2 (Chiron) and 10 ng/ml IL-7 (Preprotech). Cells were stained with anti-Vα2-PE (BD, clone B20.1), anti-CD8α-PerCP-Cy5.5 (BD, clone 53.6-7) and anti-CD45.2-APC (eBioscience, clone 104), and analyzed by flow cytometry on a CyAnADP (Beckman Coulter). Analysis was performed using Summit V4.3 software (Beckman Coulter).

Bacterial infections. Wild-type *Listeria monocytogenes* (LM) and *Listeria monocytogenes* that expresses a secreted form of OVA (LM-OVA)[40] were grown in

brain heart infusion broth (BD) to an OD_{600} of 0.1. For infections, mice were injected intravenously with 10^4 colony-forming units (CFU) LM or $2.5x10^4$ CFU LM-OVA for primary challenge and $2.5x10^5$ CFU LM-OVA for secondary challenge in HBSS. *Listeria* doses were confirmed by plating dilutions on brain heart infusion agar (BD).

Quantification and purification of barcode-labeled T cells. To quantify barcode-labeled T cells in peripheral blood samples, erythrocytes were lysed by ammonium chloride treatment and cells were stained with anti-CD8α-PE (BD, clone 53-6.7) and anti-CD45.1-APC, and analyzed by flow cytometry on a FACSCalibur (BD). To purify barcode-labeled T cells from spleen samples, spleens were homogenized through cell strainers (BD Falcon) and cells were stained with anti-Vα2-PE, labeled with anti-PE Microbeads (Miltenyi Biotec) and separated by MACS enrichment (Miltenyi Biotec).

Barcode recovery, microarray hybridizations and data analysis. Genomic DNA was isolated using a DNeasy tissue kit (Qiagen). To determine barcode sampling efficiency, barcode-containing gDNA samples were split into two equal parts (A and B) that were independently amplified by nested PCR[21]. PCR products were purified by MinElute columns (Qiagen), labeled with Cyanine-3 (Cy3) or Cyanine-5 (Cy5) fluorescent dyes (Kreatech) and hybridized to a barcode-microarray[21]. Fluorescence intensities, as quantified using ImaGene 6.0 software (BioDiscovery, Inc.) were normalized, corrected for background noise, and duplicates were averaged. Barcode dot plots depict fluorescence intensities of the hybridized A and B samples, in which each dot represents one of the 4,743 barcodes present on the barcode-microarray. Barcodes with a signal above background with $P<0.05$ were determined by one-sided *t*-test. The cut-off used for this quantification is indicated by the rectangular divider in the dot plots. The Pearson correlation between fluorescent signals of barcodes present within two samples was calculated. Calculations included a randomly drawn fraction of barcodes that were not present in a given sample (reference population), as described previously[21]. Note that the use of such a reference population within the calculations restricts correlation values to a range of -0.5 (lack of kinship) to 1 (full kinship).

CFSE labeling. Cell suspensions were washed in PBS/0.1% BSA and resuspended at $5x10^6$ cells/ml. CFSE (Molecular Probes) was added to a final concentration of 5 μM, and cells were incubated for 10 min at 37°C. Following quenching by addition of ice-cold culture medium, cells were washed in fresh medium, resuspended in HBSS, and injected intravenously into mice.

Partial splenectomy. Mice were anesthetized with isoflurane and the skin overlying the spleen was shaved and disinfected. A <1 cm incision was made in the skin and peritoneum. ¼ of the spleen was resected and the wound on the spleen was closed with Histoacryl ® Topical Skin Adhesive (TissueSeal). Thereafter, peritoneum and skin were closed with ~3 stitches and buprenorphine (0.1 μg/g body weight; Schering-Plough) was given as pain relief.

ACKNOWLEDGMENTS

We thank F. van Diepen and A. Pfauth for cell sorting; W. Brugman and R. Kerkhoven for microarray production; D. Sie for help with microarray analysis; S. Greven for animal bleeding; D. Busch (Munich, Germany) for providing LM-OVA; and D. van Heijst-Kal for theoretical discussions.

REFERENCE LIST

1. van Heijst, J. W. *et al*. Recruitment of antigen-specific CD8+ T cells in response to infection is markedly efficient. *Science* 325, 1265-1269 (2009).
2. Mercado, R. *et al*. Early programming of T cell populations responding to bacterial infection. *J. Immunol.* 165, 6833-6839 (2000).
3. Kaech, S. M. & Ahmed, R. Memory CD8+ T cell differentiation: initial antigen encounter triggers a developmental program in naive cells. *Nat. Immunol.* 2, 415-422 (2001).
4. van Stipdonk, M. J., Lemmens, E. E. & Schoenberger, S. P. Naive CTLs require a single brief period of antigenic stimulation for clonal expansion and differentiation. *Nat. Immunol.* 2, 423-429 (2001).
5. Chang, J. T. & Reiner, S. L. Protection one cell thick. *Immunity* 27, 832-834 (2007).
6. Masopust, D., Kaech, S. M., Wherry, E. J. & Ahmed, R. The role of programming in memory T-cell development. *Curr Opin Immunol* 16, 217-225 (2004).
7. Williams, M. A. & Bevan, M. J. Effector and memory CTL differentiation. *Annu Rev Immunol* 25, 171-192 (2007).
8. Reiner, S. L., Sallusto, F. & Lanzavecchia, A. Division of labor with a workforce of one: challenges in specifying effector and memory T cell fate. *Science* 317, 622-625 (2007).
9. Harty, J. T. & Badovinac, V. P. Shaping and reshaping CD8+ T-cell memory. *Nat Rev Immunol* 8, 107-119 (2008).
10. Ahmed, R., Bevan, M. J., Reiner, S. L. & Fearon, D. T. The precursors of memory: models and controversies. *Nat. Rev. Immunol.* 9, 662-668 (2009).
11. Jameson, S. C. & Masopust, D. Diversity in T cell memory: an embarrassment of riches. *Immunity* 31, 859-871 (2009).
12. van Faassen, H. *et al*. Reducing the stimulation of CD8+ T cells during infection with intracellular bacteria promotes differentiation primarily into a central (CD62LhighCD44high) subset. *J. Immunol.* 174, 5341-5350 (2005).
13. Catron, D. M., Rusch, L. K., Hataye, J., Itano, A. A. & Jenkins, M. K. CD4+ T cells that enter the draining lymph nodes after antigen injection participate in the primary response and become central-memory cells. *J. Exp. Med.* 203, 1045-1054 (2006).
14. D'Souza, W. N. & Hedrick, S. M. Cutting edge: latecomer CD8 T cells are imprinted with a unique differentiation program. *J. Immunol.* 177, 777-781 (2006).
15. Quigley, M., Huang, X. & Yang, Y. Extent of stimulation controls the formation of memory CD8 T cells. *J. Immunol.* 179, 5768-5777 (2007).
16. Stemberger, C. *et al*. A single naive CD8+ T cell precursor can develop into diverse effector and memory subsets. *Immunity* 27, 985-997 (2007).
17. Gerlach, C. *et al*. One naïve T cell, multiple fates in CD8+ T cell differentiation. *J. Exp. Med.* In press (2010).
18. Chang, J. T. *et al*. Asymmetric T lymphocyte division in the initiation of adaptive immune responses. *Science* 315, 1687-1691 (2007).
19. Ahmed, R. & Gray, D. Immunological memory and protective immunity: understanding their relation. *Science* 272, 54-60 (1996).
20. Kaech, S. M. & Wherry, E. J. Heterogeneity and cell-fate decisions in effector and memory CD8+ T cell differentiation during viral infection. *Immunity* 27, 393-405 (2007).
21. Schepers, K. *et al*. Dissecting T cell lineage relationships by cellular barcoding. *J. Exp. Med.* 205, 2309-2318 (2008).
22. Roe, T., Reynolds, T. C., Yu, G. & Brown, P. O. Integration of murine leukemia virus DNA depends on mitosis. *EMBO J.* 12, 2099-2108 (1993).

23. Panganiban, A. T. & Fiore, D. Ordered interstrand and intrastrand DNA transfer during reverse transcription. *Science* 241, 1064-1069 (1988).
24. Hu, W. S. & Temin, H. M. Genetic consequences of packaging two RNA genomes in one retroviral particle: pseudodiploidy and high rate of genetic recombination. *Proc. Natl. Acad. Sci. U S A* 87, 1556-1560 (1990).
25. Hajihosseini, M., Iavachev, L. & Price, J. Evidence that retroviruses integrate into post-replication host DNA. *EMBO J.* 12, 4969-4974 (1993).
26. Joshi, N. S. *et al.* Inflammation directs memory precursor and short-lived effector CD8(+) T cell fates via the graded expression of T-bet transcription factor. *Immunity* 27, 281-295 (2007).
27. Pearce, E. L. & Shen, H. Generation of CD8 T cell memory is regulated by IL-12. *J Immunol* 179, 2074-2081 (2007).
28. Takemoto, N., Intlekofer, A. M., Northrup, J. T., Wherry, E. J. & Reiner, S. L. Cutting Edge: IL-12 inversely regulates T-bet and eomesodermin expression during pathogen-induced CD8+ T cell differentiation. *J. Immunol.* 177, 7515-7519 (2006).
29. Curtsinger, J. M., Valenzuela, J. O., Agarwal, P., Lins, D. & Mescher, M. F. Type I IFNs provide a third signal to CD8 T cells to stimulate clonal expansion and differentiation. *J. Immunol.* 174, 4465-4469 (2005).
30. Kolumam, G. A., Thomas, S., Thompson, L. J., Sprent, J. & Murali-Krishna, K. Type I interferons act directly on CD8 T cells to allow clonal expansion and memory formation in response to viral infection. *J. Exp. Med.* 202, 637-650 (2005).
31. Badovinac, V. P., Porter, B. B. & Harty, J. T. CD8+ T cell contraction is controlled by early inflammation. *Nat Immunol* 5, 809-817 (2004).
32. Badovinac, V. P., Messingham, K. A., Jabbari, A., Haring, J. S. & Harty, J. T. Accelerated CD8+ T-cell memory and prime-boost response after dendritic-cell vaccination. *Nat Med* 11, 748-756 (2005).
33. Cho, B. K., Rao, V. P., Ge, Q., Eisen, H. N. & Chen, J. Homeostasis-stimulated proliferation drives naive T cells to differentiate directly into memory T cells. *J Exp Med* 192, 549-556 (2000).
34. Goldrath, A. W., Bogatzki, L. Y. & Bevan, M. J. Naive T cells transiently acquire a memory-like phenotype during homeostasis-driven proliferation. *J Exp Med* 192, 557-564 (2000).
35. Murali-Krishna, K. & Ahmed, R. Cutting edge: naive T cells masquerading as memory cells. *J Immunol* 165, 1733-1737 (2000).
36. Hamilton, S. E., Wolkers, M. C., Schoenberger, S. P. & Jameson, S. C. The generation of protective memory-like CD8+ T cells during homeostatic proliferation requires CD4+ T cells. *Nat Immunol* 7, 475-481 (2006).
37. Pham, N. L., Badovinac, V. P. & Harty, J. T. A default pathway of memory CD8 T cell differentiation after dendritic cell immunization is deflected by encounter with inflammatory cytokines during antigen-driven proliferation. *J Immunol* 183, 2337-2348 (2009).
38. Wong, P. & Pamer, E. G. Feedback regulation of pathogen-specific T cell priming. *Immunity* 18, 499-511 (2003).
39. Kessels, H. W., Wolkers, M. C., van den Boom, M. D., van der Valk, M. A. & Schumacher, T. N. Immunotherapy through TCR gene transfer. *Nat. Immunol.* 2, 957-961 (2001).
40. Pope, C. *et al.* Organ-specific regulation of the CD8 T cell response to Listeria monocytogenes infection. *J. Immunol.* 166, 3402-3409 (2001).